Experimental characterisation of textile compaction response: a benchmark exercise

A.X.H. Yong, A. Aktas, D. May, A. Endruweit, S.V. Lomov, S. Advani, P. Hubert, S.G. Abaimov, D. Abliz, I. Akhatov, et al.

Experimental characterisation of textile compaction response: a benchmark exercise

A. X. H. Yong[a], A. Aktas[a], D. May[b], A. Endruweit[c], S. V. Lomov[dg], S. Advani[e], P. Hubert[f], S. G. Abaimov[g], D. Abliz[h], I. Akhatov[g], M. A. Ali[i], S. Allaoui[j], T. Allen[k], D. C. Berg[h], S. Bickerton[k], B. Caglar[l], P. Causse[m], A. Chiminelli[n], S. Comas-Cardona[o], M. Danzi[p], J. Dittmann[q], C. Dransfeld[r], P. Ermanni[p], E. Fauster[s], A. George[t], J. Gillibert[j], Q. Govignon[u], R. Graupner[v], V. Grishaev[g], A. Guilloux[w], M. A. Kabachi[p], A. Keller[r], K. Kind[x], D. Large[y], M. Laspalas[n], O. V. Lebedev[g], M Lizaranzu[n], A. C. Long[c] C López[n], K. Masania[r], V. Michaud[l], P. Middendorf[q], P. Mitschang[b], S. van Oosterom[k], R. Schubnel[y], N. Sharp[z], P. Sousa[d], F. Trochu[m], R. Umer[i], J. Valette[w], J. H. Wang[aa],

[a] National Physical Laboratory, UK
[b] Institut für Verbundwerkstoffe GmbH, Germany
[c] Composites Research Group, Faculty of Engineering, University of Nottingham, UK
[d] Department of Materials Engineering, KU Leuven, Belgium
[e] Department of Mechanical Engineering and Centre for Composite Materials, University of Delaware, USA
[f] Structures & Composite Materials Laboratory, McGill University, Canada
[g] Center for Design, Manufacturing and Materials, Skolkovo Institute of Science and Technology, Russia
[h] Institute of Polymer Materials and Plastics Engineering, Technische Universität Clausthal, Germany
[i] Department of Aerospace Engineering, Khalifa University of Science and Technology, United Arab Emirates
[j] Laboratoire de Mécanique Gabriel Lamé (LaMé), Orleans University, France
[k] Centre for Advanced Composite Materials, University of Auckland, New Zealand
[l] Laboratory for Processing of Advanced Composites, Ecole Polytechnique Federale de Lausanne, Switzerland
[m] Ecole Polytechnique Montreal, Canada
[n] Materials and Components Division, ITAINNOVA, Spain
[o] Research Institute in Civil Engineering and Mechanics (GeM), University of Nantes, France
[p] Laboratory of Composite Materials and Adaptive Structures, ETH Zürich, Switzerland
[q] Institute of Aircraft Design, Universität Stuttgart, Germany
[r] Institute of Polymer Engineering, FHNW University of Applied Sciences and Arts Northwestern Switzerland, Switzerland
[s] Processing of Composites Group, Montanuniversität Leoben, Austria
[t] Department of Manufacturing Engineering, Brigham Young University, USA
[u] Institut Clement Ader, IMT Mines Albi, France
[v] Fraunhofer IGCV, Germany
[w] TENSYL, France
[x] Chair of Carbon Composites (LCC), Technische Universität München, Germany
[y] Institut de Soudure Groupe, France
[z] Composite Manufacturing and Simulation Center (CMSC), Purdue University, USA
[aa] School of Materials Science and Engineering, Wuhan University of Technology, China

Abstract

This paper reports the results of an international benchmark exercise on the measurement of fibre bed compaction behaviour. The aim was to identify aspects of the test method critical to obtain reliable results and to arrive at a recommended test procedure for fibre bed compaction measurements. A glass fibre 2/2 twill weave and a biaxial (±45°) glass fibre non-crimp fabric (NCF) were tested in dry and wet conditions. All participants used the same testing procedure but were allowed to use the testing frame, the fixture and sample geometry of their choice. The results showed a large scatter in the maximum compaction stress between participants at the given target thickness, with coefficients of variation ranging from 38 % to 58 %. Statistical analysis of data indicated that wetting of the specimen significantly affected the scatter in results for the woven fabric, but not for the NCF. This is related to the fibre mobility in the architectures in both fabrics. As isolating the effect of other test parameters on the results was not possible, no statistically significant effect of other test parameters could be proven. The high sensitivity of the recorded compaction pressure near the minimum specimen thickness to changes in specimen thickness suggests that small uncertainties in thickness can result in large variations in the maximum value of the compaction stress. Hence, it is suspected that the thickness measurement technique used may have an effect on the scatter.

Keywords: A. Fabric/textiles; D. Mechanical testing; Compressibility

1 Introduction

During the processing of fibre-reinforced composites, the fibre network is subjected to through-thickness compressive forces. These compressive forces are applied at different stages of impregnation with a liquid matrix system, depending on the processing method applied, and dictate the volume fraction of the finished component. In some processes, the reinforcement is compacted after impregnation to obtain the desired fibre volume fraction and to minimise the volume of voids in the polymer matrix. An example is filament winding, where individual fibre tows are compressed by the tension induced during the fibre deposition process on a mandrel. In pultrusion, impregnated fibre tows are compressed as they are pulled through a die. In autoclave or out-of-autoclave processing of prepregs, the impregnated fibre bed reacts to the pressure

in the autoclave or atmospheric pressure, which is applied to a vacuum bag enclosing the lay-up. On the other hand, there are processes where the dry reinforcement is compressed before it is impregnated with the matrix. In Resin Transfer Moulding, where rigid mould tools are used and the tool cavity height is given, the preform compaction response determines the reaction force on the tooling surfaces, which indicates if a given fibre volume fraction can be achieved. In vacuum infusion, where the compaction pressure is given (atmospheric pressure), the compaction response allows the component thickness and the resulting fibre volume fraction to be predicted. As high values of the fibre volume fraction, V_f, are sought after in the manufacture of structural composites to obtain high mechanical properties of the finished component, characterisation of the relation between compaction pressure and V_f of the reinforcement is vital to achieving the desired mechanical properties. Changes in V_f during preform compression also result in a reduction in its permeability, which impacts the flow of liquid resin during the subsequent preform impregnation.

From compaction experiments on carbon fibre beds impregnated with silicone oil, Gutowski et al. [1,2] found that at high fibre volume fraction ($V_f > 0.5$) the fibres carry a gradually increasing portion of the applied load, defined as the effective stress, $\overline{\sigma}$. This behaviour is caused by multiple fibre-to-fibre contacts resulting from the fibre waviness. Assuming the fibres to be curved beams in bending, the following expression was derived to express the effective stress in the fibre bed as a function of the fibre volume fraction:

$$\overline{\sigma}(V_f) = \frac{3\pi E_f \left(1 - \sqrt{\frac{V_f}{V_{f0}}}\right)}{\beta^4 \left(\sqrt{\frac{V_a}{V_{f0}}} - 1\right)^4} \qquad \text{(Equation 1)}$$

where E_f is the flexural modulus of the fibre, β is the ratio of arc length and arc height in wavy fibres (related to crimp), V_{f0} is the initial fibre volume fraction in the uncompressed preform, and V_a is the maximum achievable fibre volume fraction. The fibre bed compaction is measured by compressing a fabric stack, typically using a universal test machine (UTM) which can measure the force-displacement relationship. This type of test has been widely used to study different aspects of fibre bed compaction, and several load-volume fraction relationships have been proposed based on these studies [3-7]. Empirical or semi-empirical models derived from compaction tests are typically expressed as a power-law relation as follows:

$$V_f = a\bar{\sigma}^b \quad \text{(Equation 2)}$$

where a and b are fitting constants.

Although many aspects of fibre bed compaction have been extensively studied, there is currently no standard test procedure in place for this type of measurement. In 2016, an international survey of procedures for permeability measurement was carried out by the National Physical Laboratory (Teddington, UK) and the National Composites Centre (Bristol, UK). Responses were obtained from 34 organisations across both industry and academia, which highlighted that there is a current need for standardisation of test methods for reinforcement processing properties, permeability and compaction response [8]. Measurement standards ensure that data is traceable and comparable. In the manufacture of composite materials, standard test procedures for measurement of material properties related to processing will speed up production times by providing confidence and quality in the data used for process design. Following three international benchmark exercises on reinforcement permeability testing carried out between 2011 and 2019 [9-11], a new test standard for radial in-plane permeability measurement will be developed. However, the issue of compaction testing has not been addressed so far.

This paper reports the results of an international benchmark exercise on measurement of textile preform compaction. In this exercise, various test configurations in current use for thickness-controlled compression measurement are compared. Previous observations indicate that wet samples are typically easier to compress than dry samples due to lubrication effects [12,13], therefore the benchmark exercise was carried out for both wet and dry specimens. The reinforcement fabrics to be characterised as well as the test fluid, target thicknesses of the compressed material, and crosshead speed were initially prescribed for all users in order to isolate the effect of measurement set-up on the repeatability and reproducibility of the data. Participants had to report if they followed the instructions but had the choice in other aspects of the test, such as the sample and testing fixture geometry and testing equipment instrumentation. The aim of this study was to obtain an overview of the different approaches presently used in order to move towards a recommended test procedure for fibre bed compaction measurements by identifying aspects of the test method critical to obtaining reliable results, and assessing the degree of scatter in compression data between organisations following current methods. Table 1 lists the participants of this study.

2 Materials and Methods

2.1 Materials

Two different fabrics were used in this benchmark; a glass fibre 2/2 twill weave (in the following referred to as WOVEN) with a nominal superficial density of 295 g/m^2, supplied by Hexcel, and a biaxial (±45°) glass fibre non-crimp fabric (in the following referred to as NCF) with a nominal superficial density of 444 g/m^2, supplied by Saertex. In both cases, the material sent to participants was taken from the same batch of fabric. Further details of these fabrics can be obtained in the report for a study on permeability testing in radial flow experiments [11] which ran in parallel to this study, using the same materials. For the wet compaction tests, specimens were saturated with Dow Corning Xiameter PMX-200 silicone fluid (100 cs). Silicone oil was chosen as its viscosity is similar to that of liquid resin systems and it is often used as a test fluid in permeability measurement. This specific oil was also used in permeability benchmark exercises [10, 11]. The viscosity-temperature curve of the test fluid was characterised experimentally at TU München (a viscosity $\eta = 97$ mPa.s was measured at a temperature $T = 20$ °C).

2.2 Sample preparation

Participants were required to carry out compression tests on both fabrics, testing each under two different conditions; wet and dry. Either 10 layers of the multiaxial NCF or 14 layers of the WOVEN were compressed to a minimum thickness of 3 mm in order to achieve maximum (target) fibre volume fractions of 58 % and 54 %, respectively, as shown in Table 2. For the relatively high numbers of fabric layers used in the specimens, laying up and aligning the layers accurately may be challenging. On the other hand, different configurations of nesting between layers would be expected to cause larger scatter in results for lower numbers of layers, while convergence, i.e. smaller scatter, would be expected to be obtained at these numbers of layers. Values for the minimum thickness and the corresponding fibre volume fractions were selected as they allow the specimens to be exposed to realistic ranges (for actual composite components) of thickness and V_f during the compression tests. Each test was repeated a minimum of 5 times with a fresh specimen. Participants were asked to lay up the stacks with all layers placed in the same orientation, with the same surface facing upwards. While handling-induced fabric deformation may affect the material properties (e.g. through shear), no particular instructions were given on how to handle the fabrics to minimise this effect. To prepare specimens for the wet compaction tests, participants were asked to soak

each fabric stack in a bath of test fluid for a minimum of 15 minutes to ensure complete wet-out of the fibre bundles. Excess fluid was then drained from the wetted fabric stacks by placing them on a mesh. This step was carried out in order to minimise any effect of excess fluid on the compaction test. Following the wetting procedure, the fabric stacks were tested in compression using the same protocol as for the dry samples.

2.3 Sample and compaction platen dimensions

No recommendation was given for the dimensions of samples or compaction platens. The choice of set-up of each participant for both sample and platen shape and dimensions are shown in Table 3. Sample dimensions ranged from 50 mm to 200 mm, while platen dimensions ranged from 50 mm to 250 mm. In order to assess the effect of these dimensions on the acquired data, participants were divided into three categories. Category 1: sample area < platen area, with square (or rectangular) samples and round platens (1a), square samples and square platens (1b) and round samples and round platens (1c). Category 2: sample area > platen area, with square samples and round platens (2a), square samples and square platens (2b) and round samples and round platens (2c). Category 3: sample area = platen area, with square samples and square platens (3a) and round samples and round platens (3b). Figure 1a) and b) shows that 81 % of participants used circular platens and 65 % used square samples, making a combination of circular platens and square samples the most commonly used one. Figure 1c) presents the distribution of specimen size relative to platen size. The majority of participants (50 %) used a sample area smaller than the platen area (Category 1), 31 % had larger samples compared to the platen size (Category 2) and 15 % used equal sample and platen size (Category 3). One participant (4 %) did not fall in any of these categories.

2.4 Participant test set-up

Table 4 gives the individual test set-up details for each participant, and Table 5 lists the data acquisition and displacement control methods. The load cells used to measure the compaction force during the tests ranged from 5 kN to 250 kN in capacity. The majority of participants used a typical compression test set-up comprising of two solid stiff compaction platens, however participants 6, 8 and 9 used bespoke test rigs. Participant 8 compressed their specimens using their radial permeability test rig, which has a central hole in the upper platen for the injection of resin. Participant 9 used their through-thickness permeability test rig to carry out the compression tests, therefore specimens were constrained between porous plates within a cylinder of the same internal diameter as the specimens. Participant 6 followed a completely different

procedure using a vacuum bag to compress the specimens and measuring the specimen thickness using linear variable differential transformers (LVDTs) and the vacuum level to characterise the compaction pressure. Figure 1d) shows that 19 participants (73 %) used the UTM displacement to measure the sample thickness, while 7 participants (27 %) used LVDTs or other direct measurement techniques (laser, extensometer).

In a recent study on compression testing of a reference specimen [14], the reproducibility of results was found to be generally high for different experimental set-ups. The difference between results obtained on different UTMs was in the order of a few percent. This suggested that the influence of the test set-up on acquired pressure data was small. However, the reference specimen used in these tests had an uncompressed thickness of 68 mm and was compressed by more than 5 mm, which makes the measurements less sensitive to small uncertainties in thickness measurement. The effect of uncertainties in thickness can be expected to be more significant for compression measurement of thin specimens.

2.5 Compression profile

The participants were asked to carry out compression tests using the displacement-controlled loading profile depicted in Figure 2a). This profile required all participants to start the test with a 10 mm gap between compression platens, which ensured tests were started with zero load on the samples. The samples were compressed at a cross-head speed of 1 mm/min to a stack thickness of 3 mm and held for a period of 30 min to ensure a stable and relaxed state was captured in the results. The sample was then fully unloaded at a cross-head speed of 1 mm/min. The applied compaction force was recorded during the test. Participants were only required to carry out one compression cycle per specimen.

2.6 Machine compliance adjustment

As summarised by Sousa et al. [15], it has been reported that machine compliance can impact the precision of the values measured during compression testing. Participants were asked to record the machine compliance prior to testing by first pressing the platens together, without a sample, at a speed of 1 mm/min and recording the force at the load cell as a function of the cross-head displacement. Participants were asked to use these results to correct data for the preform compaction response. Typically, a correction would be applied according to:

$$t_t = t_{ch} + \Delta t(F_c) \quad \text{(Equation 3)}$$

where t_t is the true gap height between platens, t_{ch} is the gap height according to the cross-head displacement reading, and $\Delta t(F_c)$ is a height correction which depends on the applied compaction force, F_c. Δt can be determined from a compliance curve as shown in Figure 3a), where the compaction force, F_c, is plotted as a function of the apparent cross-head displacement, Δt. Here, a value of $\Delta t = 0$ corresponds to the point of contact between the compression plates, i.e. $F_c = 0$. Any further increase in Δt beyond the point of plate-plate contact is related to machine compliance at an applied load, F_c. For the example shown here, the relation between applied compaction force and cross-head displacement (for $\Delta t > 0$) can be expressed as:

$$F_c(\Delta t) = C\,\Delta t \quad \text{(Equation 4)}$$

where C is a compliance constant. For this specific data set, a linear approximation fits the experimental data with good accuracy (coefficient of correlation $R^2 = 0.999$). It is to be noted that the compliance curves were acquired at increasing compaction load. Because of relaxation effects, a different curve would be acquired at decreasing compaction load. $F_c(\Delta t)$ can be inverted to find:

$$\Delta t(F_c) = F_c/C \quad \text{(Equation 5)}$$

It is to be noted that the relation between F_c and Δt is in general not necessarily linear. The reported data for machine compliance displacement (Figure 3b) indicate that Δt is not negligible. The average value is Δt = 0.22 mm, which corresponds to the average maximum load in the compliance tests (F_c = 2700 N) reported by the participants. The average machine compliance displacement is of the same order of magnitude as the thickness deviation from the mean (of all participants) at maximum compaction pressure and at 10^5 Pa (Figure 3c) in the fabric compaction tests. Machine compliance displacement should ideally be at least one order of magnitude smaller than the scatter in measured thickness values for the load range experienced during the test. Furthermore, machine compliance would be expected to be linear in the range of the test, which is not the case for many participants. The non-linearity of the curves indicates an instability in the compression caused by non-controlled elements in the testing fixtures used (e.g. friction, different materials, pins, bolts, etc.).

In tests where the specimen thickness was measured using the UTM reading, the machine compliance was accounted for by applying a correction as described above to improve the accuracy of the thickness values. Most participants applied the correction to the recorded data after testing. However, some participants used

the compliance curve for calibration of the UTM prior to testing. In tests where data for the gap height was collected via a direct thickness measurement method, e.g. using LVDTs or lasers, no compliance correction needed to be applied to the specimen compaction data.

3 Results and discussion

3.1. Evaluation of recorded data

Figure 2b) shows a typical compaction curve obtained from the entire test cycle. The following information was extracted from the compaction curve as quantitative descriptors of the results: 1) maximum compaction stress, $\sigma_{c,max}$, 2) thickness at maximum compaction stress, t_{max}, 3) thickness at a compaction stress of 10^5 Pa, t_1, and 4) compaction stress at the end of the hold, $\sigma_{c,hold}$. The average value per participant for the five test repeats was calculated for each of these descriptors. It is to be noted that not all participants reached pressure values of 10^5 Pa in all test series. This was a problem particularly for the wet specimens.

Although the tests were carried out under nominally the same conditions, there is a large scatter in the data between the participants. To quantify this, minimum values, maximum values, averages and coefficients of variation (c.v.) of the descriptors described above were determined for each test series (Table 6). The percentage drop in load from the maximum compaction stress to the end of hold, ΔF_c, and its c.v. is also given in Table 6.

As a measure for the scatter in measured data for each participant individually, values for the c.v. of data for each participant are listed in Table 7. Typically, c.v. is in the order of 10 % for $\sigma_{c,max}$, and $\sigma_{c,hold}$. However, there are a few outliers with very high values of c.v., particularly for the woven fabric. The c.v. for t_{max} and t_1 is typically in the order of 1 %, indicating that the repeatability of thickness measurement for each participant is generally high. Importantly, the typical scatter in data for each participant is significantly smaller than the scatter between participants. This indicates that the scatter in data between participants is related to differences in experimental set-ups.

Table 6 shows that the thickness at a compaction stress of 10^5 Pa and the compaction stress at the end of the hold have similar coefficients of variation as t_{max} and $\sigma_{c,max}$. Therefore, the discussion will focus on t_{max}

and $\sigma_{c,max}$, as the initial compression phase to minimum thickness and maximum pressure provides sufficient information to compare compaction curves among participants. It is to be noted that the data acquired by participant 6 are not included in Tables 6 and 7 and in Figs. 4 to 6, as a different compression protocol (pressure-controlled compaction) was followed.

The coefficient of variation in maximum compaction stress (scatter between participants) for the dry tests for both fabrics was 38 %. The c.v. in the wet tests was 40 % for the NCF and 50 % for the WOVEN. Figure 4 reports the average measured maximum compaction stress and corresponding sample average thickness for both materials in dry and wet conditions. The data shows a large scatter in both stress and thickness. The range of values in compaction pressure at the sample target thickness of 3 mm is particularly large. In dry condition, the measured values range from 152 kPa to 695 kPa (average: 370 kPa) and from 63 kPa to 224 kPa (average: 114 kPa) for the NCF and WOVEN, respectively (Figure 4a) and Figure 4c)). For the wet condition, the measured maximum compaction stress is in the range from 59 kPa to 551 kPa (average: 317 kPa) and from 19 kPa to 196 kPa (average: 73 kPa) for the NCF and WOVEN, respectively (Figure 4b) and 4d)). In general, the measured compaction stress tends to be higher for the NCF than for WOVEN. This difference is related to the higher fibre volume fraction in the NCF at the target thickness. It is also a result of the difference in fabric architectures which affects the fibre mobility in fabric compression. Effects of nesting can be significant in woven fabrics, while they tend to be insignificant in NCFs. Also, there is a trend for the maximum compaction stress to be lower for wet fabric than for dry fabric, which is related to fibre lubrication. The effect of lubrication is less significant for the NCF than for WOVEN, as the fibre fixation is generally stronger in the NCF and there is a lower degree of fibre reordering.

The same trends were observed by most participants individually. However, there were a few outliers (e.g. maximum observed compaction stress higher for wet than for dry fabric), which may be related to measurement errors.

3.2 Effect of thickness measurement method

As the recorded compaction pressure near the minimum specimen thickness is very sensitive to changes in specimen thickness (Figure 2), small uncertainties in thickness can result in large variations in the maximum value of the compaction stress. In order to examine the source of the variability observed in the compaction stress, the dataset was divided into two groups based on the method used to record the sample thickness.

Figure 5 shows the data from participants using the testing machine displacement sensor (UTM) and Figure 6 shows the data for participants using calibrated LVDTs or other direct measurement methods (excluding participant 6). The results listed in Table 8 and plotted in Figs. 4 and 5 show that a similar variability in the measured compaction stress as for all participants (c.v. is 38 % to 50 %) is generally observed for the UTM group (38 % to 58 %), while the average values of $\sigma_{c,max}$ are comparable. A lower variability (10 % to 39 %) is typically observed when LVDTs or direct methods are used to measure the sample thickness (Figure 6 compared to Figure 4), while average stress values are similar (with the exception of NCF wet). However, it is to be considered that the size of the LVDT group is much smaller (7 participants) than that of the UTM group (19 participants). Carrying out a single-factor ANOVA test on the mean values obtained by each participant for $\sigma_{c,max}$ and t_{max} did not show a statistically significant effect of the thickness measurement method on the scatter in results (i.e. p-value was greater than 5%).

In general, characterisation of the machine compliance showed thickness variations in the same order of magnitude as the scatter in measured thickness values (Fig. 3c). Applying a correction to the measured thickness data to account for the compliance (in the UTM group) should eliminate the compliance as a source of scatter. However, if there is a high level of uncertainty on the compliance data (as seems to be the case for some compliance curves in Fig. 3b), there is a risk that applying a compliance correction to measured thickness data may not necessarily improve the accuracy. In these cases, the compliance may contribute significantly to the scatter in results.

To assess the compaction response independently of the large scatter in $\sigma_{c,max}$, a curve fit was applied to the raw data for the specimen thickness, t, as a function of the compaction pressure, p, acquired during the compression phase of the tests (i.e. for 0 mm to 7 mm cross-head displacement, corresponding to an experiment time from 0 min to 7 min). A power-law function was used as proposed by Robitaille et al. [3]:

$$t = Ap_n^B \qquad \text{(Equation 6)}$$

where:

$$p_n = \frac{p}{1\ \text{kPa}} \qquad \text{(Equation 7)}$$

Here, p_n is a dimensionless compaction pressure, A is the specimen thickness at $p_n = 1$, i.e. at a compaction pressure of 1 kPa, and the exponent, B, describes the shape of the curve. In some cases, curve fitting caused

problems because of the long (vertical) tail in the acquired data for t at $p_n \approx 0$, which reflects the phase of the experiment where the compression platen is not yet in contact with the specimen. To overcome this difficulty, data points were removed from the experimental curves starting at the smallest values of p_n, until a fit was found such that the coefficient of correlation, R^2, between the fit curve and the original data was greater than 0.995 (Figure 7). Average values for the constant and exponent values, A and B, respectively, are summarised in Table 9. Cases where $R^2 > 0.995$ could not be achieved are highlighted in the table. In general, the confidence in the acquired data is the higher, the more regular the curves and the better the fit. Curves of specimen thickness as a function of compaction pressure acquired by participant 10 showed strongly irregular shapes at low values of p. As a result, values for A and B derived from curve fitting using Eq. (6) are outliers. However, this appears not to have affected the maximum recorded compaction stress or the recorded minimum specimen thickness. Aiming at high accuracy in specimen thickness measurement, participant 10 used a video extensometer to track the movement of markers through a transparent Perspex frame, which enclosed the specimens. Interactions between the frame and the specimens and build-up of fluid pressure in the frame (in wet compaction) have affected the acquired data. Hence, use of this specific type of set-up is not recommended. For the remaining participants, the coefficient of variation of the constant, A, was 6 % to 8 % and ranged from 9 % to 14 % for the exponent, B. This includes one participant who carried out the compression using a vacuum bag. For each participant individually, the c.v. was typically in the range between 0 % and 4 % for A and between 0 % and 9 % for B (with only few outliers).

Figures 8 and 9 compared the fitted compaction curves between participants using the UTM and LVDT/direct displacement readings. The curves for participants using LVDT/direct sample thickness measurement appear to show less scatter compared to the UTM measurement method. This would be consistent with the latter being more prone to variability, although the machine compliance curve was applied in the reduction of the thickness data. However, as in evaluation of $\sigma_{c,max}$ and t_{max}, it is to be considered that the number of curves based on direct thickness measurement methods is smaller than the number of curves generated using UTM thickness measurement. Hence, the difference is not statistically significant. In terms of the c.v. of the parameters A and B, there appear to be trends for the c.v. of A to be higher for UTM and for the c.v. of B to be higher for LVDT/direct (Table 10). It is difficult to clearly see any difference in variability between UTM and LVDT/direct methods based on the fit parameters.

3.3. Effect of areal density

All participants determined the mass of each fabric stack, i.e. each specimen, prior to testing. This allowed the areal density of the fabrics to be calculated as an indicator for the specimen quality. Using data from the participants excluding unexplained outliers, the determined areal densities varied by 1 % for the WOVEN and 2 % for NCF. This may reflect actual local variations in material properties. Based on Equation (2), it can be estimated that this small variability in areal density, which translates into an equally small variability in fibre volume fraction, cannot be the source of the very significant variations in $\sigma_{c,max}$.

3.4. Effect of specimen and platen dimensions

For both fabrics, the dimensions of the unit cells were smaller than 10 mm, implying that even for the smallest compression platens used here (square, 50 mm × 50 mm), a representative area of the fabrics was tested. It can be argued that the dimensions of the specimens relative to the dimensions of the compression platens may have an effect on the measured pressure, as

- the specimen in-plane dimensions increase as a result of fibre straightening in the compressed reinforcement (if sample area < platen area);
- shear stresses occur in the compressed specimen around the edge of the platens (if sample area > platen area).

However, when the data are separated into groups as defined in Section 2.3 (Table 3), it is hard to identify any trends for the variability, i.e. the c.v., of the maximum pressure for each group (Table 8) at generally comparable average values (with a few outliers). This is confirmed by single-factor ANOVA analysis, which does not indicate a statistically significant effect of the specimen dimension relative to the platen dimension on the scatter in results. The c.v. of $\sigma_{c,max}$ appears to be consistently higher for circular platens than for square platens. However, there is no obvious physical explanation why the shape of the platens would have any effect on the results, particularly for set-ups where the platens are larger or equal in size to the specimens (which is the case for 69 % of participants). This apparent effect would need to be verified in a more detailed study. Table 10 shows no clear effect of shape and size of specimens and platens on the c.v. of A and B. Therefore, no conclusion can be drawn with regards to the effect of the geometry of the specimens and platens and their relative size on the measured pressure.

3.5 Effect of specimen wetting

A number of participants used a different test set-up for the wet tests to that used in the dry, which may have affected the results. However, a significant difference in c.v. was seen between the non-crimp fabric and the woven fabric. The coefficient of variation in $\sigma_{c,max}$ for WOVEN was higher in the wet tests than in the dry tests, while the c.v. was unaffected for the NCF. This is likely due to the architecture of the woven fabric, which reportedly caused difficulties during specimen preparation. The participants reported notable difficulties in handling the woven fabric, resulting in a higher degree of fraying and deformation during handling (as it has low shear resistance). The specimen wetting time for these tests was prescribed. However, a number of participants did not follow this procedure. Unlike the wetting time, the draining time for wetted specimens prior to testing was not described in the set test procedure for this benchmark. Therefore, this varied between all participants. As a result, the fluid content in the specimens at the beginning of the tests may have been variable, which may have affected the measured compaction pressure. Some participants modified the compression setup for the wet tests. One participant used a porous sinter metal structure above and below the specimens through which the oil could drain. One participant sealed the specimen in a bag with a drainage tube to allow the oil to flow away. Two participants used a perforated bottom platen and another participant placed a limiting rubber circle around the specimen, with a gap through which the oil could flow.

It is to be noted that, for wet specimens, the compaction pressure is related not only the properties of the reinforcement, but also to flow of the test fluid, which is squeezed out of the reinforcement as the specimen thickness is reduced. This effect was utilised by Buntain and Bickerton [16] and Comas-Cardona et al. [17] for continuous characterisation of the reinforcement permeability in compaction tests. Because of the relation between compaction and flow, the measured compaction pressure may depend on the speed of compaction, the reinforcement permeability (which decreases with increasing level of compaction, implying that the fluid pressure will increase during a compression test), the fluid viscosity (i.e. test temperature), and also on the specimen size, which affects the length of fluid flow paths. All participants carried out the compaction tests at room temperature, which may have varied from lab to lab. However, as the change in viscosity with temperature is relatively small in this temperature range (between η = 0.11 Pa.s at T = 15 °C and η = 0.09 Pa.s at T = 25 °C), it can be assumed that the viscosity of the test fluid was

similar for all participants. Hence, different test temperatures cannot explain the significant scatter in results. On the other hand, the dependence on specimen size may explain the larger scatter in data for the wetted specimens. It is worth pointing out that this does not contradict the observation from Section 3.2, which implied that the specimen size relative to the compaction platens does generally not have a clear effect on the measured pressure. In general, effects related to fluid flow can be minimised if the compaction speed is minimised.

3.6 Parallelism effects

Pressure calculations during compression tests assume that two parallel platens close and apply a uniformly distributed load across the compression area. If the compression platens are not parallel, the closing platens will make initial contact with the specimen on one edge, leading to an increase in apparent pressure reading while the specimen is not loaded uniformly. Similarly, lack of parallelism will affect the accuracy of zeroing the gap height between the platens. As a result, recorded curves as shown in Figure 2b) will be inaccurate. A lack of parallelism may also be a contributing factor to the irregular behaviour seen in the machine compliance tests shown in Figure 3b).

To minimise parallelism effects, participants employed a number of different strategies. Some participants tried to minimise parallelism effects during the test, others used feeler gauges to adjust the platens. One participant employed pressure sensors to check for differences in pressure distribution across the test area while one participant used a self-aligning pivot beneath the bottom platen.

To avoid lack of parallelism, it is generally helpful to use platens with a spherical seating which allows platen alignment to be adjusted. Relatively cheap pressure-sensitive film can be used to check if the pressure distribution between the platens is uniform.

3.7 Effect of load cell capacity

The load values recorded during these tests were used to calculate the compaction pressure exerted on the fabrics, therefore it was important for the load to be measured and recorded precisely. The load cell capacity for each participant varied significantly, with a range of 5 kN to 250 kN. The fraction of the load cell capacity of the recorded peak loads ranged from 0.1% to 53.8%. The accuracy of the load measurement would be influenced by how the test machine was calibrated. The calibration of each load cell is not known,

and no conclusion can be drawn. However, it is a possibility that this is a major source of variation in the data.

It is also to be considered that the total force applied to compress a specimen to a given thickness depends on the specimen area. This means that, in theory, there may be an optimum load cell capacity for each specimen size. However, in reality, the accuracy of a properly calibrated load cell is typically below 1 % of the load cell reading. In addition, linearity and repeatability are typically high, even at very low percentages of load cell capacity (typically from 0.1 % and up). Hence, the effect of the combination of load cell capacity and specimen size on the recorded data can be expected to be small.

4 Conclusions

From this benchmark exercise on characterisation of preform compaction, a number of factors which may potentially influence the outcome were identified from the participants' choices of test fixture, load and displacement measurement methods and sample geometry. Analysis of the data shows that there is a large scatter in results between participants, with coefficients of variation of maximum recorded stresses ranging from 38% to 50% for a prescribed displacement of 3 mm. This scatter is more significant than the typical scatter for each participant individually, which indicates that it is related to differences in experimental methods used.

In statistical analysis of the collected data, the large number of factors potentially affecting the measurement combined with the comparatively small size of some of the analysed sub-groups meant that it was not possible to isolate main effects on scatter from confounding factors. Nevertheless, the data suggests that the machine compliance is high for some participants, which may cause problems in terms of accuracy of results of compaction tests. Although the difference in scatter between participants who used LDVTs or other direct methods to measure the thickness and participants who used the UTM reading and applied a compliance correction was not statistically significant, the thickness measurement method may have an effect on the consistency of obtained data. Use of a power-law model to describe the compaction behaviour may be a useful way to compare results between different participants, as it considers the entire compaction

curve rather than just one point on the curve. No conclusion can be drawn with regards to the effect of the geometry of the specimens and platens and their relative size on the measured pressure.

Although it was difficult to see clear trends in the data due to the number of confounding factors, three main variables were recognised in the approach to testing and analysis between organisations; thickness measurement, approach to compliance correction and parallelism, and specimen saturation in wet compression tests. It is therefore recommended that a second benchmarking exercise be carried out in which these main parameters are defined, in order to reduce the scatter between participants, which will be necessary for the development of a standard for the measurement and characterization of compaction curve for fabrics.

Acknowledgements

The authors thank Hexcel Corporation and Saertex GmbH for supplying the materials used in this exercise free of charge. For their contribution towards the experimental work, the authors would also like to thank Jan Ivens (KU Leuven), Mohsen Orouji (Ecole Polytechnique Montreal), Damiano Salvatori and Amaël Cohades (Ecole Polytechnique Federale de Lausanne), Lucie Riffard (McGill) and Bradley Buttars and Collin Childs (Brigham Young University). Finally, the authors thank Louise Wright (National Physical Laboratory) for supporting with the statistical analysis and Argyro Martidi (National Physical Laboratory) for her contribution towards processing the data.

References

1. Gutowski TG, Kingery J, Boucher D. Experiments in composites consolidation: fiber deformation. ANTEC 86. 1986:1316-20.
2. Gutowski TG, Cai Z, Kingery J, Wineman SJ. Resin flow/fiber deformation experiments. SAMPE Q 1986,17(4):54-58.
3. Robitaille F, Gauvin R. Compaction of textile reinforcements for composites manufacturing. I: Review of experimental results. Polym Compos 1998, 19(2):198-216.

4. Chen B, Cheng A H-D, Chou T-W. A nonlinear compaction model for fibrous preforms. Composites Part A 2001, 32(5):701-707.
5. Comas-Cardona S, Le Grognec P, Binetruy C, Krawczak P. Unidirectional compression of fibre reinforcements. Part 1: A non-linear elastic-plastic behaviour, Compos Sci Technol 2007, 67(3-4):507-514.
6. Pearce N, Summerscales J. The compressibility of a reinforcement fabric. Compos Manuf 1995, 6(1):15-21.
7. Bickerton S, Buntain MJ, Somashekar AA. The viscoelastic compression behavior of liquid composite molding preforms. Composites Part A 2003, 34(5): 431-444.
8. Aktas A, Sims G, Lira C, Stojkovic M. NPL REPORT MAT 82: Survey of procedures in use for permeability measurements in liquid composite moulding processes. Teddington: National Physical Laboratory, 2016.
9. Arbter R, Beraud JM, Binetruy C, Bizet L, Bréard J, Comas-Cardona S, Demaria C, Endruweit A, Ermanni P, Gommer F, Hasanovic S, Henrat P, Klunker F, Laine B, Lavanchy S, Lomov SV, Long A, Michaud V, Morren G, Ruiz E, Sol H, Trochu F, Verleye B, Wietgrefe M, Wu W, Ziegmann G.. Experimental determination of the permeability of textiles: a benchmark exercise. Composites Part A 2011, 42(9):1157-1168.
10. Vernet N, Ruiz E, Advani S, Alms JB, Aubert M, Barbuski M, Baran B, Beraud JM, Berg DC, Correia N, Danzi M, Delavière T, Dickert M, Di Fratta C, Endruweit A, Ermanni P, Francucci G, Garcia JA, George A, Hahn C, Klunker F, Lomov SV, Long A, Louis B, Maldonado J, Meier R, Michaud V, Perrin H, Pillai K, Rodriguez E, Trochu F, Verheyden S, Wietgrefe M, Xiong W, Zaremba S, Ziegman G.. Experimental determination of the permeability of engineering textiles: Benchmark II. Composites Part A 2014, 61:172-184.
11. May D, Aktas A, Advani SG, Endruweit A, Fauster E, Lomov SV, Long A, Mitschang P, Abaimov S, Abliz D, Akhatov I, Allen TD, Berg DC, Bickerton S, Bodaghi M, Caglar B, Caglar H, Correia N, Danzi M, Dittmann J, Ermanni P, George A, Grishaev V, Kabachi MA, Kind K, Lagardère MD, Laspalas M, Liotier PJ, Park CH, Pipes RB, Pucci M, Raynal J, Rodriguez ES, Schledjewski R, Schubnel R, Sharp N, Sims G, Sozer EM, Umer R, Willenbacher B, Yong A, Zaremba S, Ziegmann

G. In-plane permeability characterization of engineering textiles based on radial flow experiments: a benchmark exercise. Composites Part A 2019, 121:100-114.

12. Kelly PA, Umer R, Bickerton S. Viscoelastic response of dry and wet fibrous materials during infusion processes. Composites Part A 2006, 37(6):868-873.
13. Kim YR, McCarthy SP, Fanucci JP. Compressibility and relaxation of fiber reinforcements during composite processing. Polym Compos 1991, 12(1):13-19.
14. May D, Kühn F, Etchells M, Fauster E, Endruweit A, Lira C. A Reference Specimen for Compaction Tests of Fiber Reinforcements. Adv Manuf Polym Compos Sci 2019, 5(4):230-233.
15. Sousa P, Lomov SV, Ivens J. Methodology of dry and wet compressibility measurement. Composites Part A 2020, 128: 105672.
16. Buntain MJ, Bickerton S. Compression flow permeability measurement: a continuous technique. Composites Part A 2003; 34(5):445-457.
17. Comas-Cardona S, Binetruy C, Krawczak P. Unidirectional compression of fibre reinforcements. Part 2: A continuous permeability tensor measurement. Compos Sci Technol 2007, 67(3–4):638-645.

Credit Author Statement

This paper was produced following the efforts of several authors. The details of each author's efforts are detailed below.

The benchmark exercise was planned and organised by:

A. X. H. Yong: writing (original draft) and writing (review and editing), formal analysis, visualization, project administration
A. Aktas: conceptualization, methodology, formal analysis, project administration, investigation
D. May: conceptualization, methodology, formal analysis, investigation

The organisers were supported by an extended Steering Committee of:

A. Endruweit: investigation, formal analysis, writing (original draft) and writing (review and editing), visualization
S. V. Lomov: investigation, formal analysis, visualization
P. Hubert: investigation, formal analysis, writing (original draft), visualization
S. Advani: writing (original draft)

Viscosity measurements for all participants were carried out by **K. Kind (investigation)**, who also participated in the benchmark.

All other authors contributed through participation in generating data for the benchmark comparison **(investigation)**:

S. G. Abaimov, D. Abliz, I. Akhatov, M. A. Ali, S. Allaoui, T. Allen, D. C. Berg, S. Bickerton, B. Caglar, P. Causse, A. Chiminelli, S. Comas-Cardona, M. Danzi, J. Dittmann, C. Dransfeld, P. Ermanni, E. Fauster, A. George, J. Gillibert, Q. Govignon, R. Graupner, V. Grishaev, A. Guilloux, M. A. Kabachi, A. Keller, D. Large, M. Laspalas, O. V. Lebedev, M Lizaranzu, A. C. Long, C López, K. Masania, V. Michaud, P. Middendorf, P. Mitschang, S. van Oosterom, R. Schubnel, N. Sharp, P. Sousa, F. Trochu, R. Umer, J. Valette, J. H. Wang,

Declaration of interests

☒ The authors declare that they have no known competing financial interests or personal relationships that could have appeared to influence the work reported in this paper.

☐The authors declare the following financial interests/personal relationships which may be considered as potential competing interests:

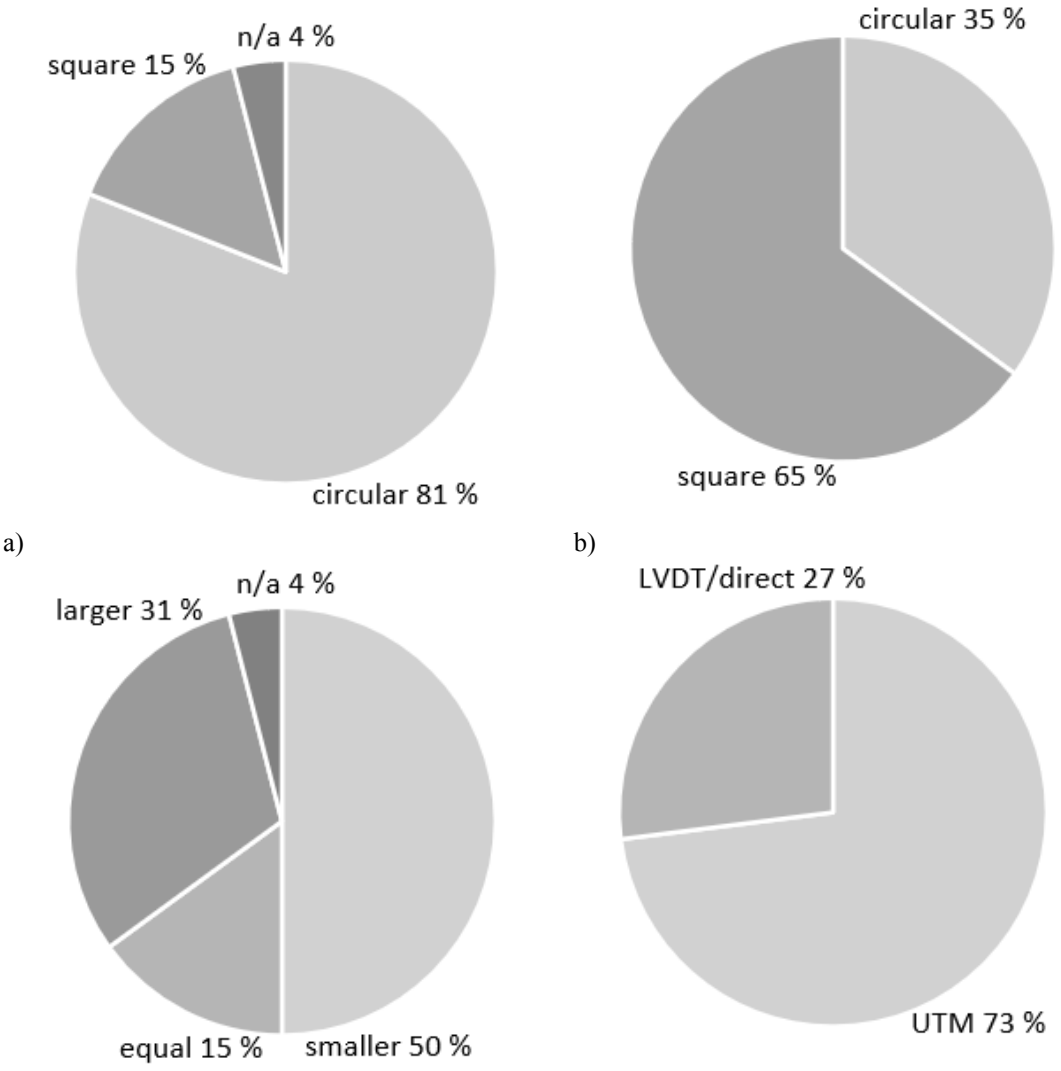

Figure 1. Participant distribution for a) Platen geometry, b) Specimen geometry, c) Specimen relative size to platen and d) Thickness measurement method.

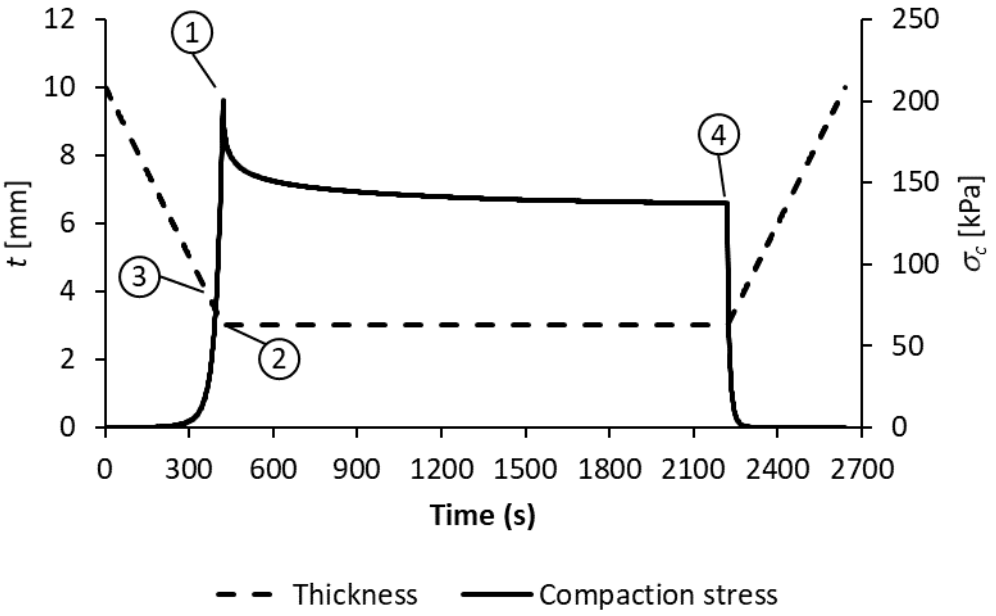

a)

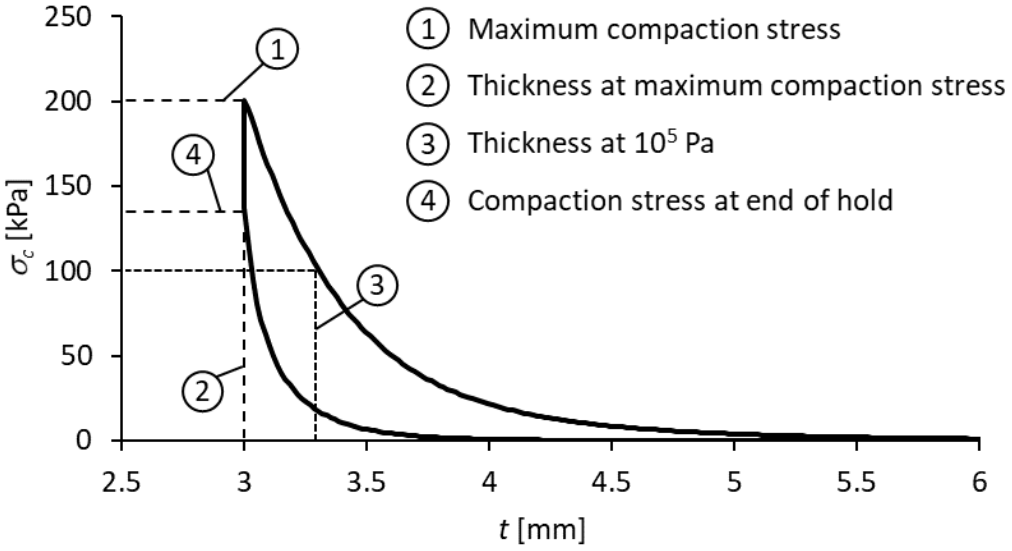

b)

Figure 2. Data from compaction experiments; a) Representative thickness and compression stress data measured by the participants, b) Data extracted from the thickness – compaction stress curve.

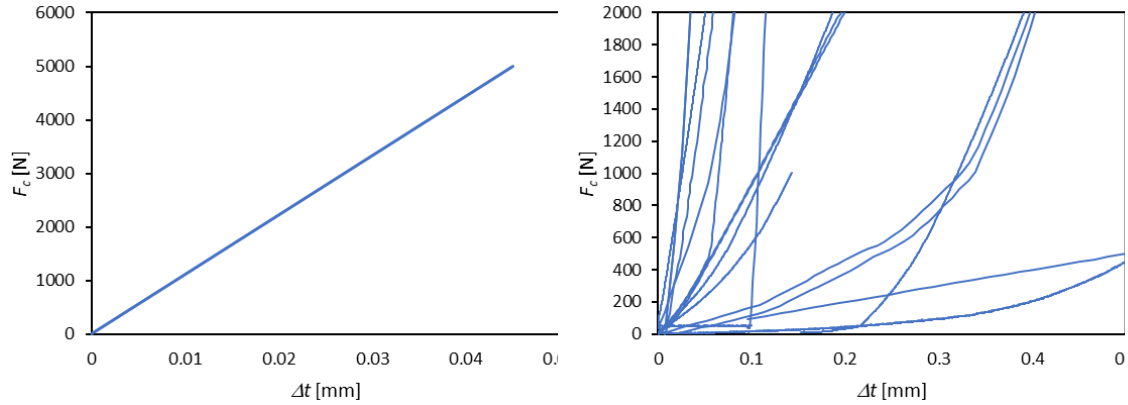

a) b)

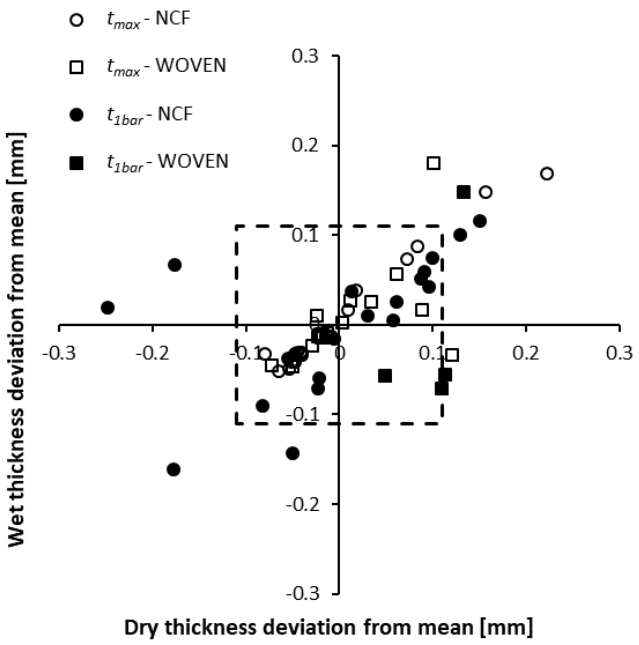

c)

Figure 3. Machine compliance characterisation; a) Example of a compliance curve for a compression plate set-up on a universal testing machine; compaction force, F_c, is a linear function of apparent cross-head displacement, Δt. b) Compliance curves measured by different participants show a wide variety of dependencies of F_c on Δt. c) Specimen thickness (maximum and at 10^5 Pa of pressure) deviation from mean for dry and wet conditions compared to the average compliance reported by the participants. The dotted line box represents the average compliance Δt = 0.22 mm for an average compaction load F_c = 2700 N.

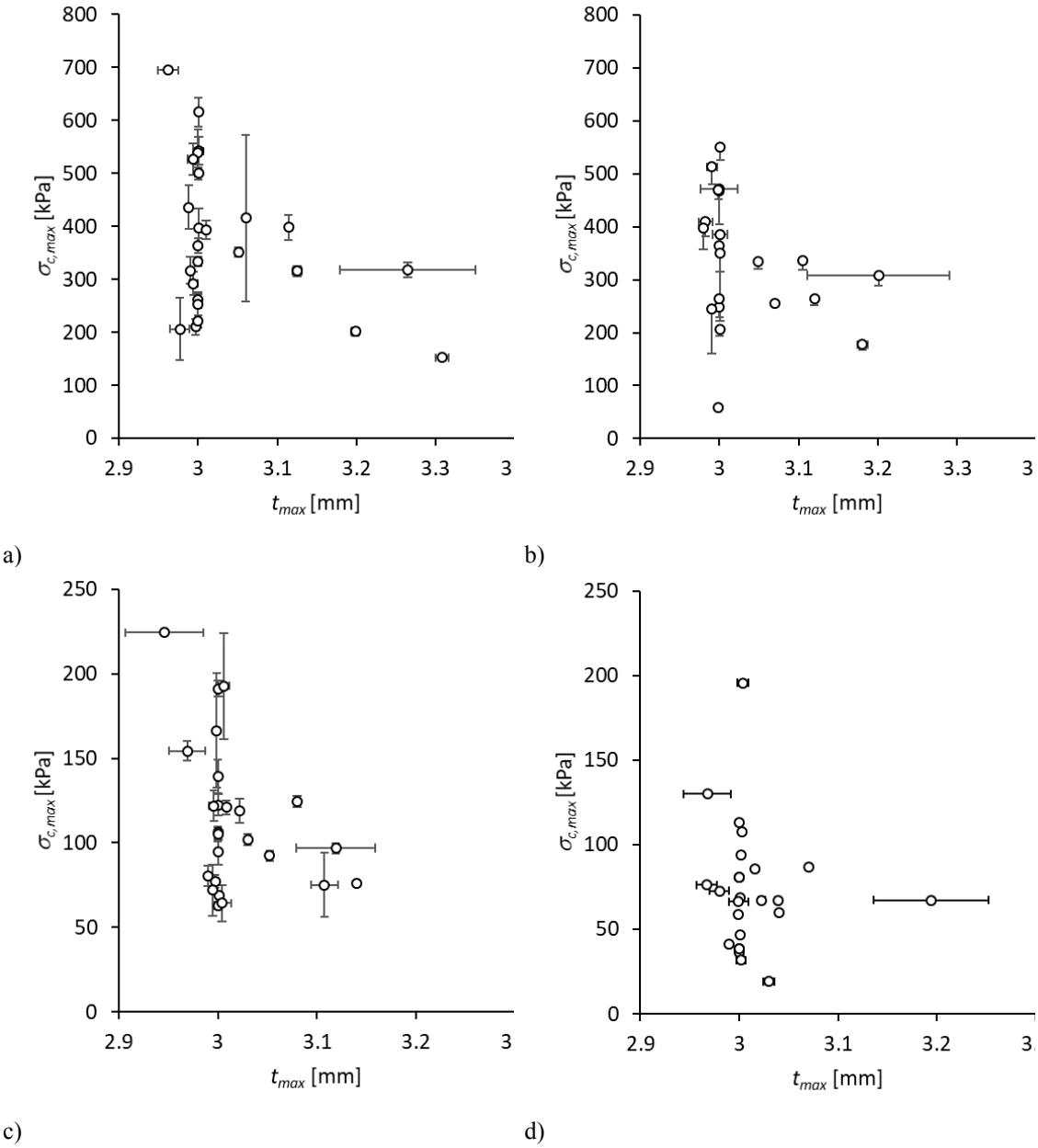

Figure 4. Maximum compaction stress, $\sigma_{c,max}$, as a function of corresponding measured thickness, t_{max}, for all participants a) NCF dry, b) NCF wet, c) WOVEN dry and d) WOVEN wet.

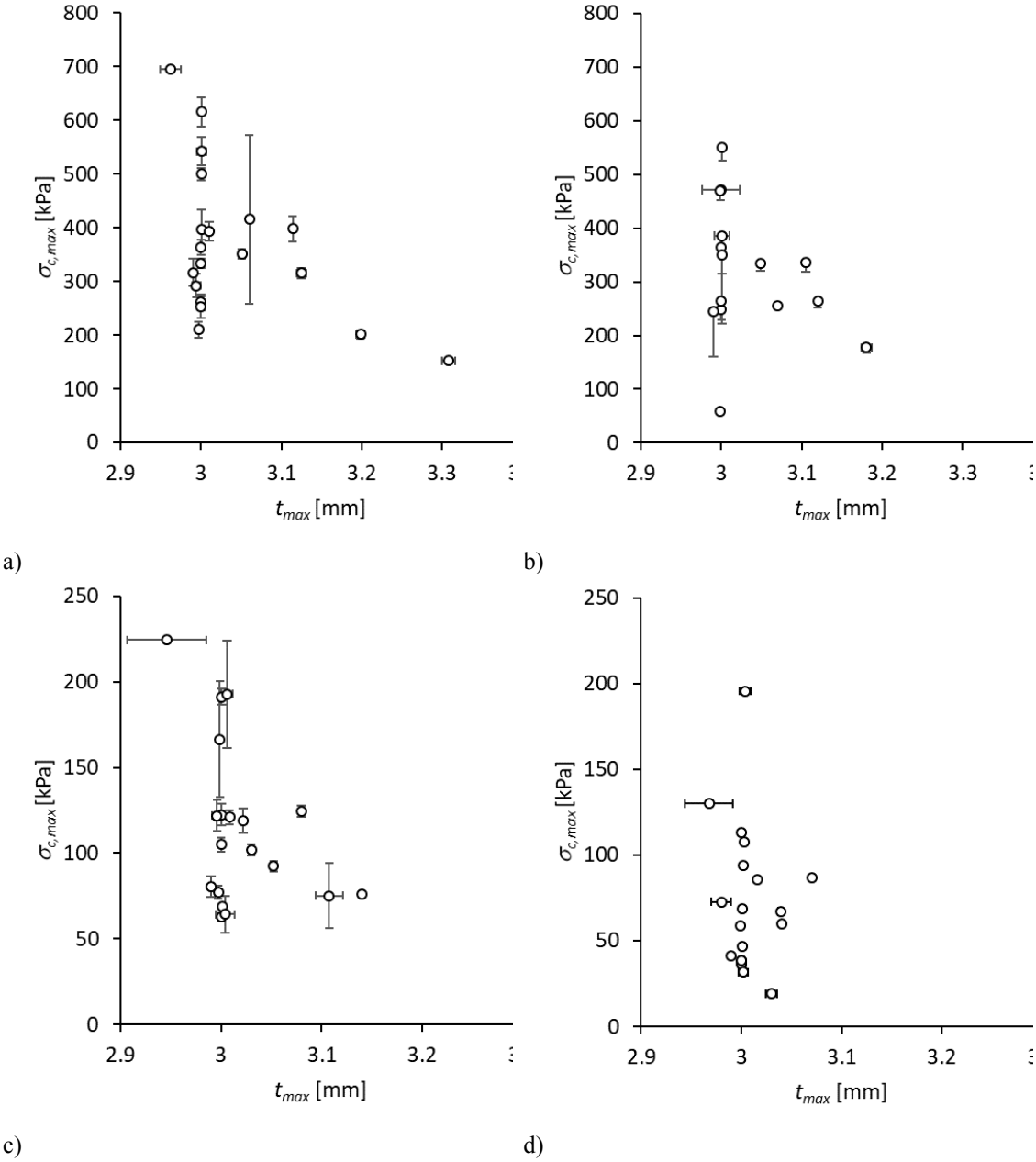

Figure 5. Maximum compaction stress, $\sigma_{c,max}$, and corresponding measured thickness, t_{max}, obtained with UTM thickness measurement for a) NCF dry, b) NCF wet, c) WOVEN dry and d) WOVEN wet.

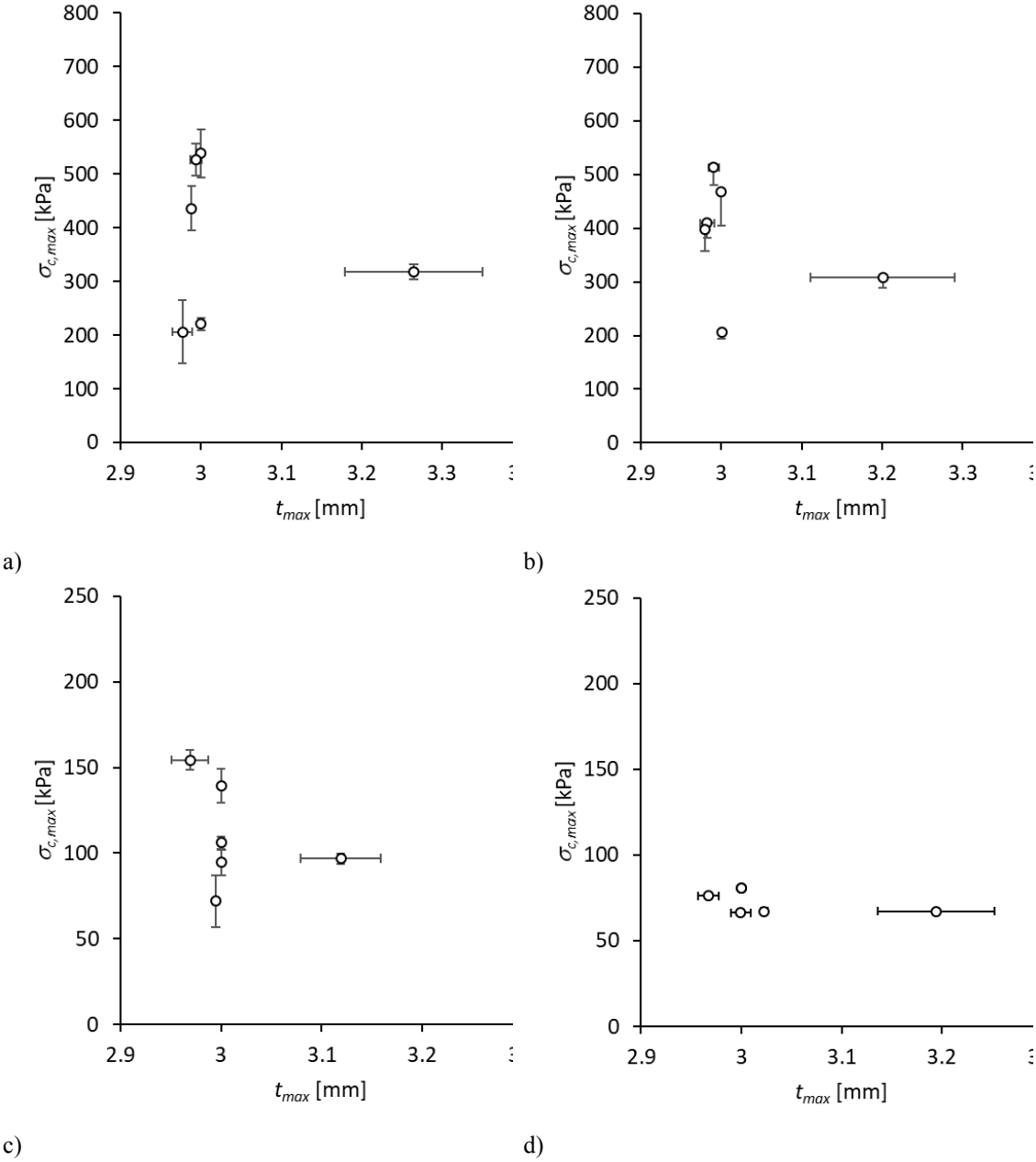

Figure 6. Maximum compaction stress, $\sigma_{c,max}$, and corresponding measured thickness, t_{max}, obtained with LVDT or other direct thickness measurement for a) NCF dry, b) WOVEN wet, c) NCF dry and d) WOVEN wet.

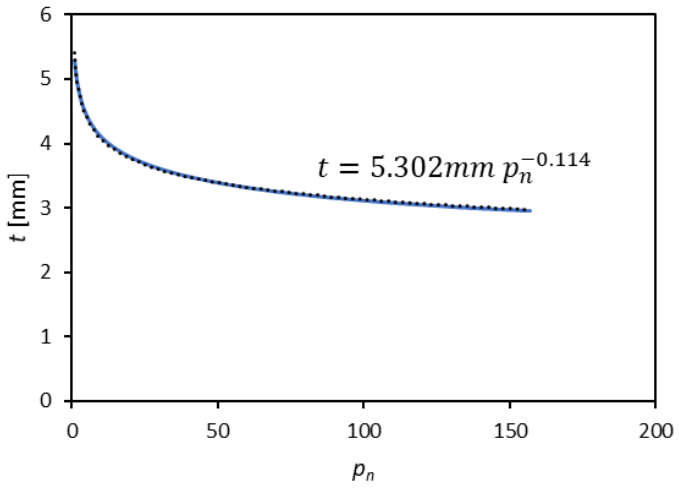

Figure 7. Specimen thickness, t, as a function of normalised compaction pressure, p_n; example of processed data allowing a power-curve to be fitted with $R^2 = 0.999$.

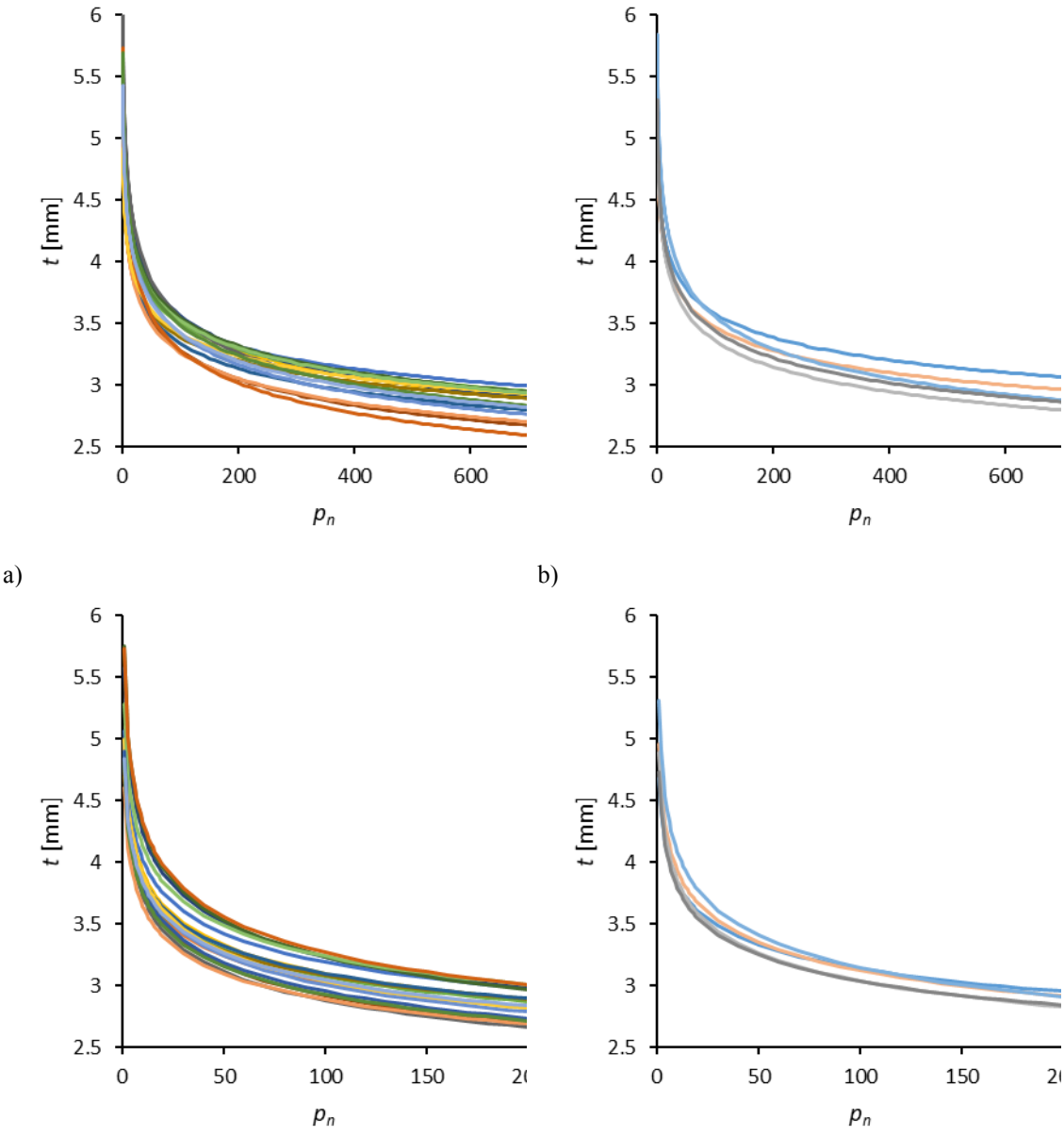

Figure 8. Fitted dry compaction curve for [thickness measurement source - material] a) [UTM - NCF dry], b) [LVDT/direct - NCF dry], c) [UTM - WOVEN dry] and d) [LVDT/direct - WOVEN dry].

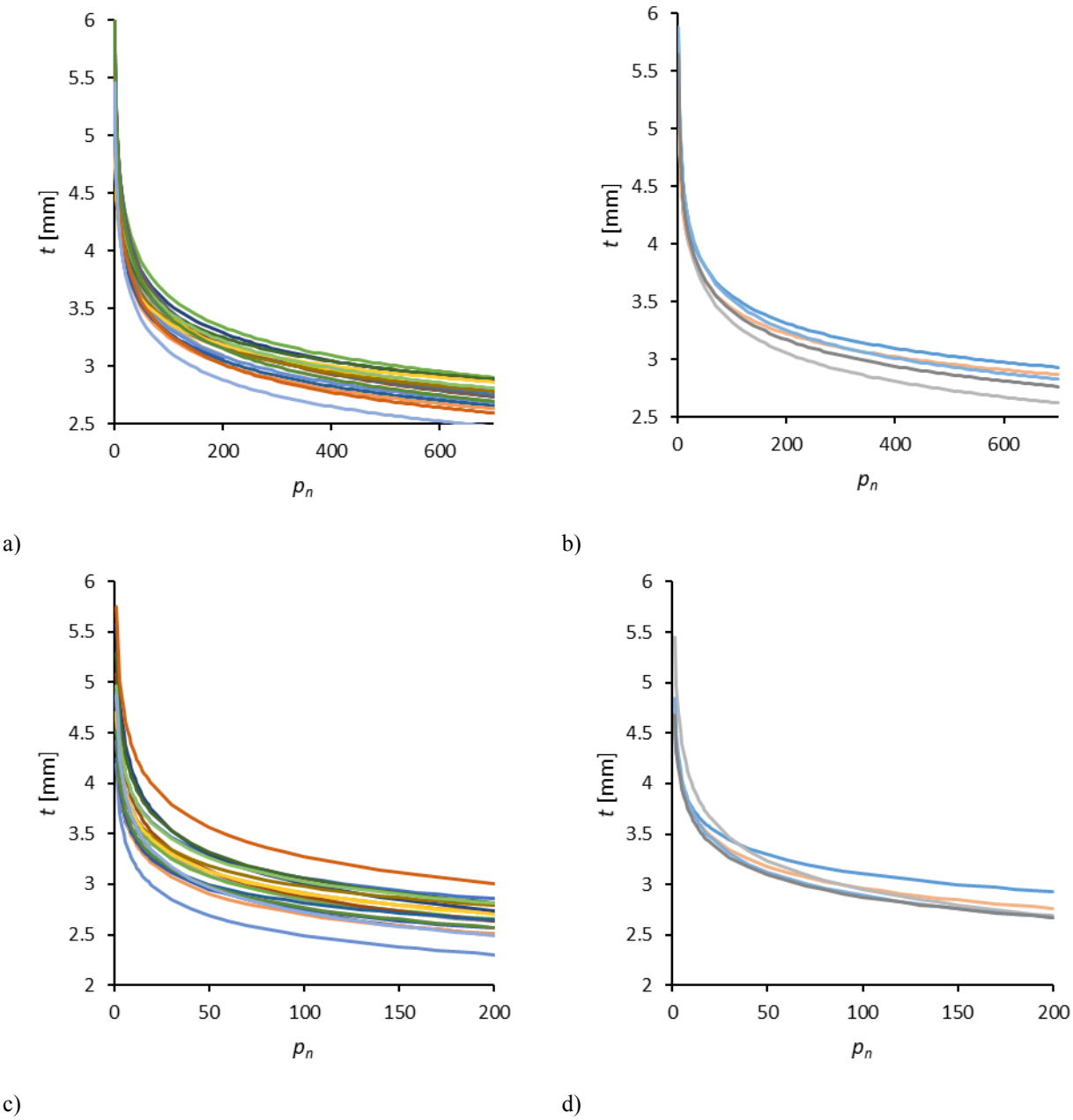

Figure 9. Fitted wet compaction curve for [thickness measurement source - material] a) [UTM - NCF wet], b) [LVDT/direct - NCF wet], c) [UTM - WOVEN wet] and d) [LVDT/direct - WOVEN wet].

Table 1: List of participants.

ID	Institution	Department	Country
1	Montanuniversität Leoben	Processing of Composites Group	Austria
2	KU Leuven	Department of Materials Engineering	Belgium
3	IMT Mines Albi-Carmaux	Institut Clément ADER	France
4	Centrale Nantes	Research Institute in Civil Engineering and Mechanics (GeM)	France
5	Orleans University	Laboratoire de Mécanique Gabriel Lamé (LaMé)	France
6	TENSYL		France
7	Institute de Soudure Composite Platform	Plateforme Composite	France
8	TU München	Chair for Carbon Composites (LCC)	Germany
9	Fraunhofer IGCV	Composite Manufacturing Engineering	Germany
10	Universität Stuttgart	Institute of Aircraft Design	Germany
11	Institut für Verbundwerkstoffe GmbH	Manufacturing Science	Germany
12	TU Clausthal	Institute of Polymer Materials and Plastics Engineering	Germany
13	Skolkovo Institute of Science and Technology	Centre for Design, Manufacturing and Materials	Russia
14	ITAINNOVA	Materials and Components Division	Spain
15	École Polytechnique Fédérale de Lausanne	Laboratory for Processing of Advanced Composites	Switzerland
16	ETH Zurich	Laboratory of Composite Materials and Adaptive Structures	Switzerland
17	FHNW University of Applied Sciences and Arts Northwestern Switzerland	Institute of Polymer Engineering	Switzerland
18	University of Nottingham	Composites Research Group, Faculty of Engineering	UK
19	National Physical Laboratory	Materials Testing Group	UK
20	Wuhan University of Technology	School of Materials Science and Engineering	China
21	University of Auckland	Centre for Advanced Composite Materials	New Zealand
22	Khalifa University of Science and Technology	Department of Aerospace Engineering	UAE
23	McGill University	Structures and Composite Materials Laboratory	Canada
24	École Polytechnique Montréal	Department of Mechanical Engineering	Canada
25	Brigham Young University	Department of Manufacturing Engineering	USA
26	Purdue University	Composites Manufacturing and Simulation Center	USA

Table 2: Guidelines for sample stack preparation.

Preform	Number of layers in a fabric stack	Minimum compacted thickness [mm]	Maximum fibre volume fraction	Number of test repeats (minimum)	
				Dry	Wet
NCF	10	3	58 %	5	5
WOVEN	14	3	54 %	5	5

Table 3: Specimen and platen dimensions of each participant.

ID	Code	Sample		Platen	
		Shape	Dimensions [mm]	Shape	Dimensions [mm]
1	2a	Square	60 x 60	Circular	50 Ø
2	2a	Square	90 x 90	Circular	70 Ø
3	2a	Square	NCF: 160 x 160 WOVEN: 170 x 170	Circular	150 Ø
4	2a	Square	180 x 180	Circular	150 Ø
5	1a	Square	100 x 100	Circular	140 Ø
6	n/a	Square	95 x 95 NCF Dry: 143 x 143	n/a	n/a
7	1a	Square	150 x 150	Circular	300 Ø
8	2a	Square	280 x 280	Circular	250 Ø
9	2a	Circular	199 Ø	Circular	200 Ø
10	3b	Square	80 x 80	Rectangular	80 x 80
11	1c	Circular	100 Ø	Circular	120 Ø
12	2b	Square	55 x 55	Square	50 x 50
13	1a	Circular	100 Ø	Circular	203 Ø
14	1c	Circular	120 Ø	Circular	135 Ø
15	3a	Square	100 x 100	Square	100 x 100
16	2a	Square	150 x 150	Circular	Dry: 135 Ø Wet: 120 Ø
17	2c	Circular	150 Ø	Circular	136 Ø
18	1c	Circular	80 Ø	Circular	90 Ø
19	1c	Circular	132 Ø	Circular	150 Ø
20	1a	Square	100 x 100	Circular	200 Ø
21	1a	Square	100 x 100	Circular	230 Ø
22	1c	Circular	100 Ø	Circular	150 Ø
23	1b	Square	50 x 50	Rectangular	80 x 55
24	1a	Square	100.2 x 100.2	Circular	157 Ø
25	3c	Circular	150 Ø NCF dry: 150 x 150	Circular	150 Ø
26	1a	Square	101.6 x 101.6	Circular	150 Ø

Table 4: Test setup for each participant.

ID	Machine	Load cell capacity	Press material	Drainage method
1	EuroTest	200 kN	Steel	Drainage channel
2	Instron	5 kN	Steel	Free to flow
3	Instron	30 kN	Steel	Free to flow
4	Instron	100 kN	Steel & aluminium	Perforated bottom platen
5	Instron	10 kN	Steel	Free to flow
6	Vacuum pump	N/A	Vacuum bag	N/A
7	Schenck	40 kN	Steel	Free to flow
8	Hegewald & Peschke	100 kN	Aluminium & glass	Free to flow
9	Hegewald & Peschke	250 kN	Steel	Porous sinter metal structures above and below specimen
10	Hegewald & Peschke	25 kN	Steel	Gap at sample borders

11	Zwick	100 kN	Steel	Free to flow
12	Zwick	0 -10 kN	Steel	Free to flow
13	Instron	250 kN	Steel	Opening in limiting rubber circle
14	Zwick	100 kN	Steel	Free to flow
15	Walter + Bai	10 kN	Steel	Free to flow
16	Zwick	100 kN	Steel	Immersed
17	Zwick	100 kN	Steel	Free to flow
18	Instron	50 kN	Steel	Free to flow
19	Instron	100 kN	Steel	Free to flow
20	Reger	30 kN	Steel	Perforated and grooved bottom platen
21	Instron	Auto Ranging	Aluminium & glass	Free to flow
22	Instron	5 kN	Steel	Free to flow
23	MTS	5 kN	Aluminium	Sealed with drainage tube
24	Instron	100 kN	Steel	Free to flow
25	Instron	5 kN	Aluminium	Free to flow
26	MTS	22 kN	Steel	Free to flow

Table 5: Methods for displacement control and thickness measurement for each participant. Where thickness was measured using UTM readings, a compliance correction was typically applied to the data after testing. Some participants used a compliance correction for machine calibration prior to compression testing. These are labelled with an asterisk (*).

ID	Closing control	Thickness measurement
1	LVDT	LVDT
2	UTM	UTM
3	UTM	UTM
4	UTM	UTM
5	UTM	UTM
6	LVDT	LVDT
7	UTM	UTM
8	UTM	Laser
9	UTM*	UTM
10	UTM	Video extensometer
11	UTM*	UTM
12	UTM	UTM
13	Strain gauge extensometer	Strain gauge extensometer
14	UTM	UTM
15	UTM	LVDT
16	UTM	UTM
17	UTM	UTM
18	LVDT	LVDT
19	UTM	UTM
20	UTM	UTM
21	UTM*	UTM
22	UTM	UTM
23	UTM	UTM
24	UTM	UTM
25	UTM	UTM
26	UTM	UTM

Table 6: Measured values for maximum compaction stress, $\sigma_{c,max}$, thickness at maximum compaction stress, t_{max}, thickness at a compaction stress of 10^5 Pa, t_1, and compaction stress at the end of the hold, $\sigma_{c,hold}$. Scatter of values between participants. Minimum value, maximum value, average and coefficient of variation are given based on the average values for each participant. The average percentage drop of load from maximum to end of hold, ΔF_c, and its coefficient of variation are also given.

Test series	$\sigma_{c,max}$				t_{max}				t_1				$\sigma_{c,hold}$				ΔF_c	
	min [kPa]	max [kPa]	average [kPa]	c.v.	min [mm]	max [mm]	average [mm]	c.v.	min [mm]	max [mm]	average [mm]	c.v.	min [kPa]	max [kPa]	average [kPa]	c.v.	average	c.v.
NCF (dry)	152	695	370	38 %	2.96	3.31	3.04	3 %	3.20	3.60	3.45	3 %	125	505	230	37 %	36 %	23 %
NCF (wet)	59	551	317	40 %	2.98	3.20	3.03	2 %	3.00	3.54	3.39	4 %	33	311	196	38 %	37 %	22 %
WOVEN (dry)	63	224	114	38 %	2.95	3.14	3.02	2 %	3.02	3.25	3.12	2 %	52	182	91	37 %	20 %	22 %
WOVEN (wet)	19	196	73	50 %	2.97	3.19	3.01	1 %	3.04	3.26	3.11	3 %	14	146	50	58 %	33 %	23 %

Table 7: Measured values for maximum compaction stress, $\sigma_{c,max}$, thickness at maximum compaction stress, t_{max}, thickness at a compaction stress of 10^5 Pa, t_1, and compaction stress at the end of the hold, $\sigma_{c,hold}$. Scatter in measured values for each participant. Minimum, maximum and average values of coefficient of variation for each participant are given.

Test series	$\sigma_{c,max}$			t_{max}			t_1			$\sigma_{c,hold}$		
	min c.v.	max c.v.	average c.v.	min c.v.	max c.v.	average c.v.	min c.v.	max c.v.	average c.v.	min c.v.	max c.v.	average c.v.
NCF (dry)	0 %	38 %	7 %	0 %	3 %	0 %	0 %	3 %	1 %	1 %	32 %	7 %
NCF (wet)	0 %	42 %	8 %	0 %	3 %	0 %	0 %	5 %	1 %	1 %	43 %	9 %
WOVEN (dry)	0 %	25 %	7 %	0 %	1 %	0 %	0 %	3 %	1 %	2 %	25 %	8 %
WOVEN (wet)	0 %	76 %	11 %	0 %	2 %	0 %	0 %	3 %	1 %	2 %	101 %	13 %

Table 8: Maximum compaction stress, $\sigma_{c,max}$, for groups of participants selected based on thickness measurement method, platen geometry, specimen geometry, and specimen size relative to platen. Average values and coefficients of variation are given.

Variable	Case	NCF dry		WOVEN dry		NCF wet		WOVEN wet	
		average [kPa]	c.v.	average [kPa]	c.v.	average [kPa]	c.v.	average [kPa]	c.v.
Thickness measurement method	UTM	369	38 %	115	41 %	297	43 %	73	58 %
	LVDT/Direct	374	39 %	111	28 %	383	29 %	73	10 %
Platen geometry	Circular	389	36 %	118	38 %	319	42 %	77	50 %
	Square	272	30 %	92	25 %	311	31 %	55	44 %
Specimen geometry	Circular	424	34 %	125	32 %	342	49 %	74	34 %
	Square	340	39 %	108	42 %	304	34 %	73	59 %
Specimen size relative to platen	Larger	428	36 %	129	32 %	273	56 %	75	38 %
	Equal	323	64 %	109	51 %	351	48 %	80	28 %
	Smaller	349	30 %	106	40 %	334	29 %	70	65 %

Table 9: Values of constant, *A*, and exponent, *B*, in fit curves for each participant and test series. Test series where the coefficient of correlation between measured data and fit curves was smaller than 0.995 are indicated with an asterisk (*). Test series where problems with the set-up resulted in irregular curves and poor quality of the fit are indicated with ($^{+}$).

	NCF Dry		NCF Wet		WOVEN Dry		WOVEN Wet	
ID	*A* [mm]	*B*	*A* [mm]	*B*	*A* [mm]	*B*	*A* [mm]	*B*
1	5.04	-0.08	5.30	-0.09	4.96*	-0.10*	4.70*	-0.10*
2	5.52	-0.10	5.38	-0.10	5.75	-0.12	5.29	-0.12
3	5.11	-0.08	5.71	-0.11	5.07	-0.10	4.91	-0.10
4	4.92	-0.08	5.01	-0.09	5.00	-0.11	4.71	-0.10
5	5.50	-0.10	5.32	-0.10	4.90	-0.11	4.41	-0.10
6	4.81	-0.07	5.09*	-0.09*	4.54	-0.08	4.80*	-0.11*
7	5.32	-0.10	6.22	-0.13	4.95*	-0.11*	5.09*	-0.12*
8	5.20*	-0.09*	5.82	-0.12	4.89	-0.10	5.45	-0.13
9	5.79	-0.11	5.87	-0.11	5.58	-0.12	5.58	-0.13
10	6.01^{+}	-0.13^{+}	9.03^{+}	-0.20^{+}	8.85^{+}	-0.25^{+}	$^{+}$	$^{+}$
11	4.93	-0.08	5.40	-0.10	4.69	-0.09	4.60	-0.09
12	5.50	-0.10	5.71	-0.11	4.97	-0.10	4.69	-0.10
13	5.31	-0.09	5.64	-0.11	4.74	-0.10	4.68	-0.11
14	6.14	-0.12	6.26	-0.13	4.82	-0.11	4.82*	-0.12*
15	5.16	-0.08	5.57	-0.10	4.68	-0.09	4.59	-0.08
16	5.43	-0.10	5.46	-0.12	4.84	-0.10	4.87	-0.13
17	5.24	-0.09	6.06	-0.11	4.84	-0.10	4.69*	-0.11*
18	5.84	-0.11	5.87	-0.11	5.31	-0.11	4.84	-0.11
19	5.43	-0.09	5.74	-0.11	5.28	-0.11	4.97	-0.11
20	5.69	-0.11	6.09	-0.12	4.81	-0.11	4.52	-0.11
21	5.55	-0.10	5.76	-0.11	4.76	-0.10	4.64	-0.10
22	5.06	-0.09	5.46	-0.11	4.88	-0.10	4.25*	-0.09*
23	5.65	-0.11	5.55	-0.11	4.97	-0.11	4.19	-0.11
24	5.11	-0.10	5.38	-0.11	4.60	-0.10	4.41	-0.11
25	5.27	-0.09	5.88*	-0.12*	4.99	-0.11	4.85	-0.12
26	5.73	-0.12	5.73	-0.12	5.74	-0.12	5.74	-0.12

Table 10: Coefficients of variation of fit curve parameters, *A* and *B*, for groups of participants selected based on thickness measurement method, platen geometry, specimen geometry, and specimen size relative to platen.

Variable	Case	NCF dry		WOVEN dry		NCF wet		WOVEN wet	
		c.v. (A)	c.v. (B)	c.v. (A)	c.v. (B)	c.v. (A)	c.v. (B)	c.v. (A)	c.v. (B)
Thickness measurement method	UTM	6 %	12 %	7 %	8 %	6 %	9 %	9 %	11 %
	LVDT/Direct	6 %	13 %	5 %	10 %	4 %	10 %	7 %	17 %
Platen geometry	Circular	6 %	12 %	7 %	8 %	6 %	10 %	8 %	11 %
	Square	5 %	16 %	3 %	11 %	2 %	7 %	6 %	14 %
Specimen geometry	Circular	7 %	12 %	6 %	7 %	5 %	7 %	7 %	13 %
	Square	5 %	13 %	7 %	9 %	6 %	11 %	9 %	12 %
Specimen size relative to platen	Larger	4 %	9 %	6 %	8 %	6 %	12 %	6 %	11 %
	Equal	6 %	14 %	9 %	15 %	3 %	11 %	10 %	22 %
	Smaller	6 %	11 %	6 %	8 %	5 %	7 %	9 %	10 %